Published in final edited form as:
*Neurobiol Aging*. 2014 May ; 35(5): 1162–1176. doi:10.1016/j.neurobiolaging.2013.10.077.

# Pomegranate juice exacerbates oxidative stress and nigrostriatal degeneration in Parkinson's disease

**Victor Tapias, PhD**[1,2], **Jason R. Cannon, PhD**[3], and **J. Timothy Greenamyre**[1,2,4]

Victor Tapias: tapiasvm@upmc.edu; Jason R. Cannon: cannonjr@purdue.edu

[1]Department of Neurology, University of Pittsburgh, Pittsburgh, PA 15260, USA

[2]Pittsburgh Institute for Neurodegenerative Diseases, University of Pittsburgh, Pittsburgh, PA 15260, USA

[3]School of Health Sciences, Purdue University, West Lafayette, IN 47907, USA

[4]Pittsburgh VA Healthcare System, Pittsburgh, PA 15206, USA

## Abstract

Numerous factors contribute to the death of substantia nigra (SN) dopamine (DA) neurons in Parkinson's disease (PD). Compelling evidence implicates mitochondrial deficiency, oxidative stress, and inflammation as important pathogenic factors in PD. Chronic exposure of rats to rotenone causes a PD-like syndrome, in part by causing oxidative damage and inflammation in SN. Pomegranate juice (PJ) has the greatest composite antioxidant potency index among beverages, and it has been demonstrated to have protective effects in a transgenic model of Alzheimer's disease. The present study was designed to examine the potential neuroprotective effects of PJ in the rotenone model of PD. Oral administration of PJ did not mitigate or prevent experimental PD but instead increased nigrostriatal terminal depletion, DA neuron loss, the inflammatory response, and caspase activation, thereby heightening neurodegeneration. The mechanisms underlying this effect are uncertain, but the finding that PJ *per se* enhanced nitrotyrosine, inducible nitric oxide synthase, and activated caspase-3 expression in nigral DA neurons is consistent with its potential pro-oxidant activity.

### Keywords

Parkinson's disease; mitochondria; oxidative stress; inflammation; pomegranate juice; polyphenols; rotenone; neuroprotection; neurotoxicity



**Corresponding author:** John Timothy Greenamyre, MD, PhD, University of Pittsburgh, 3501 Fifth Avenue, Suite 7039, Pittsburgh, PA 15260, Tel: 001-412-648-9793, Fax: 001-412-648-9766, jgreena@pitt.edu.



**Disclosure Statement**

There are no actual or potential conflicts of interest, including any financial, personal or other relationships with people or organizations during the development of the work submitted.

## 1. INTRODUCTION

Selective degeneration of dopamine (DA) neurons in the substantia nigra (SN) underlies the cardinal motor impairments of Parkinson's disease (PD). The pathogenesis of PD is associated with mitochondrial dysfunction and increased oxidative stress which may be caused in part by selective inhibition of complex I activity (Beal, 2005; Hu et al., 2010). Decreased activity and immunoreactivity of complex I have been observed in the SN of PD patients (Schapira et al., 1989) along with increased oxidative modification of lipids, proteins, DNA, and RNA (Jenner, 2003). Free radicals and other reactive oxygen species (ROS) and reactive nitrogen species (RNS) derived from DA metabolism and auto-oxidation (Cadet and Brannock, 1998), nitric oxide reactions (Beckman et al., 1990), lipid peroxidation (Liang et al., 2007), impaired mitochondrial function (Tapias et al., 2009), and alterations in defensive endogenous antioxidant systems (Chinta et al., 2007) may all lead to oxidative and nitrosative stress, contributing to a progressive loss of DA neurons. In this context, antioxidant strategies confer neuroprotection in several animal models of PD (Liang et al., 2007; Tapias et al., 2009). Evidence also suggests that microglial activation may perpetuate DA neuron degeneration, and anti-inflammatory therapies that inhibit microglial activation are protective in experimental PD (Wu et al., 2002; Wu et al., 2009).

Polyphenols are the major class of phytochemicals in pomegranate fruit and reportedly have antioxidant activity in PD models *in vivo* (Guo et al., 2007) and *in vitro* (Levites et al., 2002). The antioxidant activity of phenolic compounds is due to their ability to scavenge free radicals, donate hydrogen atoms, and chelate metal ions. Specifically, the antioxidant capacity of pomegranate juice (PJ) is mainly attributed to punicalagin and has been shown to be 3 times higher than that of red wine or green tea infusion (Gil et al., 2000). In addition, PJ has favorable pharmacological properties and may protect against inflammation, cancer and neurodegeneration (Hartman et al., 2006; Koyama et al., 2010).

Systemic administration of rotenone reproduces behavioral, anatomical, and neuropathological changes occurring in idiopathic PD (Betarbet et al., 2000; Cannon et al., 2009). Uniform inhibition of mitochondrial respiratory chain complex I across brain regions by rotenone stimulates widespread oxygen free radical formation and $NO^{\bullet}$ production (He et al., 2003) but degeneration is selective for the DA nigrostriatal system. Evidence suggests that microglia play a pivotal role in rotenone-induced degeneration of DA neurons (Sherer et al., 2003a).

This study was undertaken to determine whether dietary supplementation with PJ provides neuroprotective effects after rotenone exposure. We have focused our attention on the effect of PJ because its key components cross the blood-brain barrier, it is easy to administer, and it is safe. Because oxidative stress and inflammation may be prominent in PD pathogenesis (McGeer et al., 1988; Wu et al., 2002) we hypothesized that PJ would be protective.

## 2. MATERIALS AND METHODS

### 2.1. Animals

Six-seven-month-old adult male Lewis rats were used for all experiments (Hilltop Lab Animals, Inc., Scottdale, PA, USA). The animals were maintained under standard conditions of 12 h light/dark cycle, 22±1 °C temperature-controlled room and 50–70% humidity, and were provided water and food *ad libitum*. They were adapted for two weeks to the conditions described above before experimentation. All studies were approved by the Institutional Animal Care and Use Committee at the University of Pittsburgh and were performed in accordance with published NIH guidelines.

### 2.2. Experimental design

Animals were randomly divided into the following 4 groups: vehicle+vehicle (VEH+VEH), pomegranate juice+vehicle (PJ+VEH), vehicle+rotenone (VEH+ROT), and pomegranate juice+rotenone (PJ+ROT). The experimental groups were comprised of 6 animals for vehicles (VEH+VEH and PJ+VEH) and 11 animals for rotenone groups (VEH+ROT and PJ +ROT). Prior to injections, body-weights were recorded for each animal.

Rotenone (Sigma-Aldrich, St. Louis, MO, USA) was administered intraperitoneally once a day at a dose of 3.0 mg/kg until the end of the treatment. The solution was prepared as a 50x stock dissolved in pure dimethyl sulfoxide (DMSO) at final concentration of 2%, then diluted in a medium chain fatty acid called Miglyol 812N at final concentration of 98% (Sasol North America, Inc., Houston, TX; distributed by Warner Graham, Baltimore, MD, USA), and administered at 1 mL/kg. This regimen produces relatively uniform bilateral nigrostriatal lesions, leading to loss of about 50% of DA neurons (Cannon et al., 2009). Control animals received an equivalent amount of vehicle (2% DMSO+98% Miglyol).

Rats were pretreated with PJ (POM Wonderful; Los Angeles, CA) administered in their drinking water for two weeks. PJ from a single lot of PJ concentrate was diluted 1:40 in filtered water; importantly, this dose was selected after careful review of a manuscript that showed no statistically significant differences for any behavioral or neuropathological assessments between different concentrations of PJ (Hartman et al., 2006). The PJ used in our study is four times more concentrated than other conventional PJ sold commercially; thus, the final concentration of PJ at 1:40 dilution does not significantly differ from non-concentrated PJ.

The rats drank between 6.5–7.5 mL of fluid per day. The estimated polyphenol content in PJ is 3600 μg/mL (Aviram et al., 2008); thus, the amount of polyphenols consumed by the rats was estimated to be ~ 0.6–0.7 mg/day. The juice mixture was made fresh two-three times per week, filtered and administered until the end of the study. Control rats (VEH+VEH) received sugar water that matched the sugar content of the 1:40 PJ dilution (85% sucrose, 7.5% D-(+)-glucose, and 7.5% D-fructose).

### 2.3. Behavioral study

**2.3.1. Rearing behavior analysis—**As a functional measure of loss of nigral DA neurons, spontaneous rearing activity was evaluated. Animals were placed in a clear Plexiglas cylinder (height = 30 cm, diameter = 20 cm) for 5 min. While in the cylinder, animals typically rear and engage in exploratory behavior by placing their forelimbs along the wall of the cylinder (Schallert and Tillerson, 2000). All animals were observed and video recorded under red-light (10 lx), to encourage movement. To be classified as a rear, the animal had to raise the forelimbs above shoulder level and make contact with the cylinder wall with either one or both forelimbs. Removal of a forelimb from the cylinder wall and contact with the bottom surface of the cylinder was required before another rear was scored. Rearing behavior was assessed at baseline and again after 5 days of rotenone or vehicle injection for each rat. Importantly, this test has been used to assess bilateral DA-dependent behavioral deficits in the rotenone model (Cannon et al., 2009).

**2.3.2. Postural instability test—**To evaluate postural stability – a hallmark feature of PD (Woodlee et al., 2008) – rats were held almost vertically facing downward while one forelimb was allowed to contact the table surface which was lined with medium-grit sand paper. The tip of the rat's nose was aligned with the zero line of a ruler. One forelimb was gently restrained against the animal's torso by the experimenter allowing the rat to plant its unrestrained forelimb. The rat was then moved forward over the single planted forelimb

until it made a “catch-up” step to regain its center of gravity. The new position of the tip of the nose indicated the displacement of the body needed to trigger a catch-up step in the unrestrained supporting forelimb. The postural instability test was carried out at baseline and after 5 days of rotenone treatment. In divergence with unilateral 6-OHDA models of PD, here, both forelimbs were averaged together because rotenone produces bilateral symptoms. This test has been previously used in rotenone-treated rats to assess bilateral deficits (Cannon et al., 2009).

### 2.4. Brain tissue processing

Tissue collection was carried out when the animals had reached endpoint which was empirically determined for each individual animal when the behavioral phenotype became debilitating, i.e., when akynesia, rigidity, and postural instability were manifested. Animals were euthanized by $CO_2$ inhalation followed by decapitation. The brains were quickly removed and sectioned sagittally along the midline. One hemisphere was fixed in 4% paraformaldehyde for 7 days and then placed in 30% sucrose in PBS for cryoprotection until infiltration was complete (at least three days). The striatum and SN from the other half of the brain were dissected on ice, flash frozen in liquid nitrogen and then stored at −80 °C until they were processed for neurochemical or immunoblotting analysis, respectively.

### 2.5. Neurochemistry

Striatal levels of DA and its metabolites, DOPAC (3,4-dihydroxyphenylacetic acid) and HVA (homovanillic acid) were analyzed using high-performance liquid chromatography with electrochemical detection (HPLC-ECD) (Cannon et al., 2009; Tapias et al., 2010). Frozen striatal tissue samples were suspended in cold 0.1 N $HClO_4$ (perchloric acid) and 0.01 % $C_6H_8O_6$ (ascorbic acid) and homogenized by microtip sonication. The suspension was centrifuged at 16,100×*g* for 30 min at 4 °C to sediment cell debris and undissolved material. The supernatant was then collected and filtered in Costar Spin-X 0.22 μM nylon membrane polypropylene centrifuge tubes at 1,000×*g* and then stored at −80 °C. The supernatant was then injected into a Waters 2695 HPLC separation module (Waters Corp., Milford, MA, USA) using an autosampler within the module and the sample temperature was maintained at 4 °C. The HPLC mobile phase contained 0.06 M sodium phosphate monobasic, 0.03 M citric acid, 8% methanol, 1.075 mM 1-octanesulfonic acid, 0.1 mM ethylenediaminetetraacetic acid, and 2 mM sodium chloride, at pH 3.5. Chromatography was isocratic with a flow rate of 1.0 mL/min. Neurotransmitters were separated on a Waters XBridge C18 4.6×150 mm column with a 3.5 μm particle size and detected on a Waters 2465 electrochemical detector with a glassy carbon electrode set at 750 mV referenced to an ISAAC electrode. The separation and detection occurred at 28 °C. Neurotransmitters were determined as ng of neurotransmitter/metabolite per mg protein and quantified using a standard curve generated from injection of standards of the highest available purity. Protein concentration in the tissue samples was determined by the Bradford (Bio-Rad; Hercules, CA, USA) protein assay method in a 96-well plate.

### 2.6. Immunohistochemistry

Coronal sections from brains were cut on a frozen sliding microtome at 35 μm, collected and stored in cryoprotectant (1 mL 0.1 M phosphate ion ($PO_4^{3-}$) buffer, 600 g sucrose, and 600 mL ethylene glycol, pH = 7.2) at −20 °C until use. Brain sections were initially rinsed in PBS 6 times 10 min to remove the cryoprotectant. Unless otherwise specified, all incubations were carried out at RT. A sequence of incubation steps was done in 3% hydrogen peroxide for 10 min, then in 10% normal donkey serum in PBS containing 0.3% Triton X-100 (Thermo Fisher Scientific #bp151; Pittsburgh, Pennsylvania, USA) for 1 h, and rinsed with PBS (3×for 10 min each) between each step.

To label DA neurons for stereological assessment, the sections were incubated in a primary mouse monoclonal antibody for TH (1:3000; Millipore #MAB318; Bilerica, MA, USA) for 72 h at 4 °C plus 2 h at RT to attain optimal antibody penetration. After rinses in PBS (3×10 min), sections were incubated for 1 h in biotinylated donkey anti-mouse secondary antibody (1:200, Jackson Immuno Research #81685; West Grove, PA, USA) and subsequently placed in a solution containing Avidin-Biotin Peroxidase Complex (ABC Elite kit; Vectastain, Vector Labs; Burligame, CA, USA) for 1 h. Finally, after washing in 3 changes of PBS, the reaction was developed in 3,3′ diaminobenzidine tetrahydrochloride solution (DAB, Vector Labs; Burligame, CA, USA) for 5 min. At the end of the incubations, the sections were mounted onto pluscoated slides using Aquamount (Lerner Labs, Pittsburgh, PA, USA).

For sections used for general histology, the tissue was air-dried at RT, dehydrated using an alcohol gradient and Histoclear (National Diagnostics, Atlanta, GA, USA), then coverslipped using Histomount (National Diagnostics).

To measure striatal TH density by infrared immunofluorescence, the sections were rinsed 6×in PBS for 10 min each and subsequently blocked for 1 h with 10% normal donkey serum in PBS with 0.3% Triton X-100. Next, sections were incubated in a primary mouse monoclonal antibody for TH (1:2000; Millipore #MAB318; Bilerica, MA, USA) at 4 °C for 72 h. Following incubation, sections were rinsed in 3 changes of PBS for 10 min each and incubated for 1 h with IRDye 800 secondary antibody (1:500, LI-COR Biosciences #92632212; Lincoln, NE, USA). The sections were washed for 3×10 min in PBS and then mounted directly onto pluscoated slides and coverslipped using gelvatol mounting media.

For oxidative and nitrosative stress evaluation, nigral sections were washed 3×in PBS for 10 min and pre-incubated for 5 h with 1% Triton X-100 in PBS at 4 °C. The samples were rinsed 3×with PBS. Antigen retrieval using a pepsin digest solution (Invitrogen Life Technologies; Carlsbad, CA, USA) was carried out for 5 min at 37 °C. After one rinse in PBS, non-specific binding sites were blocked for 1h. Sections were incubated for 72 h at 4 °C with primary antibody: polyclonal sheep anti-TH antibody (1:2000; Millipore #AB1542), polyclonal rabbit anti-NT (1:500; Millipore #06-284) and monoclonal mouse anti-4-HNE (1:500; OxisResearch #24327; USA). After an additional incubation for 1 h, SN sections were rinsed in 3 changes of PBS and then incubated in a secondary antibody solution for 2 h: Alexa 488 anti-sheep antibody (1:500; #A11015, Invitrogen), Cy3 anti-rabbit antibody (1:500; #711-165-152, Jackson ImmunoResearch; West Grove, PA, USA), and 647 anti-mouse antibody (1:500; #A31571, Invitrogen). Following 3 washes in PBS for 10 min each, tissue sections were then mounted directly onto pluscoated slides and coverslipped using Aquamount (Lerner labs).

Confocal microscopy was utilized to evaluate neuroinflammatory responses in the SN. The staining procedure was identical to that describe above for oxidative and nitrosative stress, except that the pepsin digestion step was omitted. Briefly, sections were stained with a polyclonal sheep anti-TH antibody, a monoclonal mouse anti-iNOS (1:5000; Abcam #ab49999; Cambridge, MA, USA) and a polyclonal rabbit anti-Iba1 (1:25000; Wako #019-19741; Richmond, VA, USA).

### 2.7. Nitrotyrosine and 4-hydroxynonenal determination by confocal immunofluorescence

Brain SN sections were processed to study the role of oxidative and nitrosative stress in the rotenone-induced pathogenesis of PD. Five coronal SN sections per animal were immunostained with two different antibodies that specifically recognize nitrotyrosine and 4-hydroxynonenal. Fluorescent images were captured using a confocal microscope (Olympus BX61, Fluoview 1000; Melville, NY, USA) and quantification was carried out at 40x. A

total of 200-300 $TH^+$ neurons from 4 different animals per group were ratiometrically analyzed and data from each tissue section were combined to determine means.

### 2.8. Dopaminergic immunoreactivity of inducible nitric oxide synthase and ionized calcium binding adaptor molecule 1 (microglia marker)

Neuroinflammatory responses were analyzed in nigral DA neurons by immunochemistry. Five SN serial sections from 4 rats per group were labeled using anti-$TH^+$ and anti-iNOS or anti-Iba1 antibodies and appropriate fluorescently conjugated secondary antibodies. Quantification for iNOS was performed on confocal images at 40x. An average of 200–300 DA neurons was examined.

The motorized stage technique recently developed and reported by our lab (Tapias et al., 2012) was utilized to determine Iba1 values. Briefly, immunofluorescence images of the SN from rat brain sections were acquired on an automated Nikon 90i microscope equipped with a linear encoded motorized stage at 20x. The entire surface of the SN was scanned using NIS-Elements software and acquired images were exported to ImageJ software. Average particle size, number of microglial-positive cells, and total area were determined through the SN.

### 2.9. Infrared fluorescence intensity measurements of striatal TH

Serial TH immunopositive-labeled sections were scanned at 800 nm at a resolution of 21 μm and a 3 (arbitrary unit) sensitivity setting on an Odyssey infrared-imager (LI-COR Biosciences, Lincoln, NE, USA) as previously described (Tapias et al., 2010). Briefly, striatal sections (3–5 from each animal) were used to generate the reported average striatal DA fiber intensity. Care was taken to avoid saturation of the fluorescence intensity. Using the V 3.0 Odyssey Software, the dorsal striatum was outlined and the average pixel intensity for each section was obtained.

### 2.10. Unbiased stereology

The number of SN TH-immunoreactive neurons from one hemisphere, including pars compacta and pars reticulata, was estimated stereologically using an optical fractionator unbiased sampling design equipped with a Zeiss Axioskop 2 plus microscope hard-coupled to a MAC 5000 controller module, a high-sensitivity 3CCD video camera system (CX 9000, MBF Biosciences, Williston, VT, USA), and a Pentium IV PC workstation. An experimenter blinded to the treatment group performed all analyses. The thickness of the sections was measured by focusing on the top of the section, setting the Z-axis to 0, and then refocusing to the bottom of the section and recording the actual thickness.

An entire nigral series was arbitrarily selected and every sixth section was sampled through the entire SN, which resulted in the analysis of 10–13 sections per animal. The sections were analyzed for counting using a 100x oil immersion objective and only the cells with a visible nucleus that was clearly TH-immunopositive were counted. The counting frame was 45×45×13 μm (height×width×dissector height) and the sampling grid was 125×125 μm. The average final section thickness was 22.67 μm, making the average guard zone 4.8 μm from the top and bottom of the section. Stereological parameters were optimized based on a pilot study in both control and rotenone-treated animals to produce a rigorous estimate of nigral DA neurons. The CE Gunderson (m = 1) values were < 0.1 for all animals.

### 2.11. Immunoblotting

SN brain tissue was homogenized in ice-cold stringent RIPA lysis buffer (1:30 w/v) by sonication. Proteins were quantified using the Bradford assay, and lysates were either used immediately or stored at −80 °C. Respective lysates were then incubated with precipitant

solution (50% acetone, 25% pure ethanol, and 25% methanol) and cleared by centrifugation at 13,200×rpm for 10 min at 4 °C. The pellets were resolved in 4x reducing loading buffer and were boiled for 3 min at 100 °C.

Equal amounts of protein from each lysate were separated by 4–12% gradient SDS-PAGE gels and electrotransferred onto nitrocellulose membranes, followed by immunoblotting with the indicated primary antibodies diluted in blocking buffer solution (#927-40000, LI-COR): mouse monoclonal anti-IL-1β (1:1000; #MABF18, Millipore), mouse monoclonal anti-COX-2 (1:500; #358200, Invitrogen), rabbit polyclonal anti-TNF-α (1:500; #04-1114, Millipore), or rabbit polyclonal anti-NF-κB p65 (1:1000; #ABE347, Millipore) were used to study inflammatory conditions and responses. Furthermore, in order to examine cell death (apoptosis), primary antibodies were directed against rabbit polyclonal anti-caspase-3 (1:1000; #9962, Cell Signaling, Danvers, MA, USA) and rabbit polyclonal anti-activated caspase-3 (1:1000; #9961L, Cell Signaling).

The membranes were then incubated with respective infrared conjugated secondary antibodies for 1 h at RT and rinsed four times with PBS. Densitometry of positively stained bands was quantified using a LI-COR Odyssey infrared imaging system. The optical density of each protein band was normalized to β-actin, used as internal control. The graphs represent the average of the ratios calculated from four different animals in triplicate.

### 2.12. Statistical analysis

Statistical comparisons between two groups were analyzed by using unpaired Student's *t*-test. Multisample testing was performed using one-way ANOVA analysis followed by the Newman-Keuls post-hoc test. The log-rank test was used for comparison of survival curves. Data are expressed as mean and standard error of the mean (S.E.M.). $p < 0.05$ was considered significant for all tests. GraphPad Prism 5 software was utilized for statistical analysis.

## 3. RESULTS

### 3.1. Weight and survival curves

Body weights (Fig. 1A) and survival rates (Fig. 1B) were similar across treatment groups with no statistically significant differences. Animals that died during the treatment were excluded from analysis (n = 2).

### 3.2. Behavioral deficits

To examine whether neuroprotection by PJ could result in behavioral improvement, the rats were trained and tested for behavioral analyses (Fig. 2). In control animals (n = 6), PJ did not affect rearing behavior (Fig. 2A); however, animals treated with rotenone (n = 11) exhibited fewer rears when tested on the fifth day after the first daily rotenone injection compared to controls ($p < 0.001$). The degree of behavioral impairment was greater in rats that received PJ and rotenone in combination ($p < 0.05$). A second behavioral measure, postural instability, was not affected by PJ administration in control rats (Fig. 2B). Although there was a trend toward difference between groups, postural instability did not significantly differ in animals that received PJ and rotenone compared to animals treated with rotenone alone. Postural stability was significantly different in rats after 5 days treatment with rotenone relative to controls ($p < 0.01$).

### 3.3. DA and metabolites

Changes in catecholamine levels were measured by HPLC in the striatum (Fig. 3). Administration of rotenone to rats led to a substantial depletion of striatal DA levels

compared to vehicles (Fig. 3A; $p < 0.01$). Although the concentrations of DOPAC and HVA were unchanged (Fig. 3B and 3C), the turnover rate was significantly increased (Fig. 3D, $p < 0.05$). Supplementation with PJ had no effect on the catecholamine pool.

### 3.4. Striatal tyrosine hydroxylase immunohistochemistry

TH-immunoreactive fibers emanate from DA neurons in the SN and ramify extensively throughout the entire striatum. Immunohistochemical analysis showed that 3.0 mg/kg/day of rotenone induced severe loss of striatal TH-immunopositive DA fibers (Fig. 4). Although PJ alone (Fig. 4E-H) did not have any effect on TH-immunoreactive fibers compared to VEH +VEH animals (Fig. 4A-D) it appeared to potentiate striatal terminal loss relative to the rotenone group (Fig. 4I-L) when PJ was administered together with rotenone (Fig. 4M-P), as there was an additional diffuse loss of terminals outside the overt focal lesion (dorsolateral area). Immunofluorescence staining was performed and analyzed on the Odyssey near-infrared imaging system to quantify terminal density (Fig. 4Q). Quantification of the intensity of immunostained striatal TH-positive projections (Fig. 4R) revealed that DA fiber depletion was more severe with PJ administration in rotenone-treated animals compared to VEH+ROT rats (378 ± 30 vs 474 ± 34 fluorescent units; $p < 0.05$).

### 3.5. Nigral dopaminergic cell loss

To determine whether PJ might protect against rotenone-induced loss of nigral DA neurons, midbrain sections were stained for TH immunoreactivity (Fig. 5). Consistent with the depletion of DA terminals in the striatum, rotenone induced significant DA neuronal death compared to vehicle treatment (Fig. 5Q; 12,950 ± 744 vs 21,430 ± 878 DA neurons/hemisphere; $p < 0.001$). High magnification images of the dorsolateral region of SN revealed that dietary supplementation with PJ not only failed to attenuate rotenone-induced loss of nigral DA neurons and fiber pruning but actually potentiated the rotenone insult (Fig. 5O and 5P vs 5K and 5L). As noted, rotenone-treated rats had 12,950 ± 744 DA neurons per hemisphere, but animals that received PJ+ROT had significantly fewer DA neurons (8,833 ± 397; $p < 0.05$). Together with the striatal TH immunohistochemistry (Fig. 5), our data demonstrate that PJ potentiates nigrostriatal DA neurotoxicity induced by rotenone.

### 3.6. Oxidative and nitrosative insult in substantia nigra dopaminergic neurons

We studied the effect of PJ on tyrosine nitration and lipid peroxidation (Fig. 6) within nigral DA neurons ($TH^+$ staining, white). Immunofluorescent micrographs at 100x depicted a faint NT fluorescence signal (Fig. 6B) and weak 4-HNE staining (Fig. 6C) in the SN of vehicle rats. The staining for NT was significantly increased after oral administration of PJ to the rats (Fig. 6F). Rotenone treatment induced higher NT immunoreactivity (Fig. 6J) and increased 4-HNE fluorescence intensity to an even greater extent (Fig. 6K). The combination of PJ+ROT led to an additive increase in fluorescence signal for NT (Fig. 6N), but not for 4-HNE (Fig. 6O).

The quantification of the relative fluorescence for NT is shown in Fig. 6Q. A significant increase in NT levels occurred in PJ+VEH conditions compared to VEH+VEH ($p < 0.05$). Rotenone exposure produced a significant elevation of NT levels compared to the vehicle group ($p < 0.01$), which was exacerbated when rotenone was co-administered with PJ ($p < 0.001$). Figure 6R depicts the overall assessment for 4-HNE immunoreactivity. Enhanced 4-HNE labeling was observed after rotenone treatment relative to the vehicle group ($p < 0.001$), but no differences were detected between PJ+ROT and VEH+ROT animals. Together, these findings demonstrate a pro-oxidant effect of PJ in the rotenone model of PD.

### 3.7. Microglial activation: Ionized calcium binding adaptor molecule 1 expression

Fluorescence immunohistochemical examinations at 40x magnification and 4x zoomed images demonstrated that Iba1 is expressed only in microglia (Fig. 7). Administration of PJ alone (Fig. 7C and inset 7D) did not alter Iba1 expression compared to vehicle (Fig. 7A and inset 7B). The most prominent differences in microglial morphology (ramified and amoeboid phenotype) were observed in response to rotenone induced-toxicity (Fig. 7E and inset 7F); a significant increase in "particle size" indicated microglial activation in the SN of rats. Nonetheless, no additive effects were found with PJ (Fig. 7G and inset 7H). Quantification of particle size (Fig. 7I), number of Iba1 positive cells (Fig. 7J), and total area occupied by the microglia (Fig. 7K) were performed.

### 3.8. Modulation of proinflammatory mediators in nigral dopaminergic neurons

Induction of iNOS is thought to contribute to DA neuron demise (Liberatore et al., 1999). Confocal images at 100x revealed a lack of iNOS in the control group (Fig. 8A2). Increased iNOS immunoreactivity in $TH^+$ neurons and the neuropil was observed when PJ was administered to the rats compared to the vehicle group (Fig. 8A5). The expression of iNOS was significantly enhanced in response to rotenone treatment (Fig. 8A8) in contrast to vehicle groups. Upregulation of iNOS-positive cells was even greater after PJ and rotenone in combination (Fig. 8A11). Fluorescence levels of iNOS were quantified (Fig. 8A13); juice consumption induced iNOS activation relative to VEH+VEH group ($p < 0.05$). The neurotoxin rotenone increased the expression of iNOS above the vehicle and PJ values ($p < 0.001$). Co-administration of PJ and rotenone dramatically raised iNOS immunoreactivity compared to the rotenone-alone group ($p < 0.01$).

To examine the possible proinflammatory role of PJ, we also studied the expression of the cytokine interleukin-1β (IL-1β), the enzyme cyclooxygenase-2 (COX-2), tumor necrosis factor-α (TNF-α), and nuclear factor kappa B (NF-kB) subunit p65 in the SN of rats exposed to rotenone (Fig. 8B and 8C). Western blots showed that PJ administration did not modify COX-2 expression (Fig. 8B2). IL-1β protein levels were also unaffected in response to the combination of PJ and rotenone (Fig. 8B3). Supplementation with PJ failed to reduce the expression of the inflammatory cytokine TNF-α (Fig. 8C3). However, PJ administration resulted in a robust increase in the p65 catalytic subunit of the transcription factor NF-kB (~ 58% increase after quantification of both bands; $P < 0.01$) after rotenone injury (Fig. 8C2). Values were obtained as means of raw data and presented as arbitrary units (A.U.) of optical density along with the corresponding S.E.M. These findings suggest that PJ may contribute to changes in inflammatory gene expression via the NF-kB pathway.

### 3.9. Caspase-3 activation

Mitochondrial dysfunction and oxidative damage may result in caspase activation. Lysates of SN tissue were processed for immunoblotting using antibodies against caspase-3 and cleaved caspase-3 (Fig. 9). Markedly enhanced caspase-3 activation was observed in the PJ +VEH group relative to the VEH+VEH group (272.7 ± 26.8 vs 99.37 ± 7.3 respectively, $p < 0.05$). Cleaved caspase-3 was activated even to a greater extent after rotenone treatment (VEH+ROT). Although no statistically significant differences were observed between the VEH+ROT and PJ+ROT groups, the level of activated caspase-3 was raised ~ 1.5-fold following PJ administration (388.2 ± 64.4 vs 555.8 ± 86.5; n = 4). Results were expressed as percentage changes relative to vehicle group (VEH+VEH). Optical densities were given in arbitrary units and were obtained by the ratio of cleaved caspase-3 to total caspase-3 protein.

### 3.10. Fluid consumption and sugar intake

Supplemental Figure 1A shows that rats treated with PJ and rotenone consumed less water compared to all other groups ($p < 0.01$) – in a small proportion and only the last few days of life. The sugar intake levels (Supplemental Fig. 1B) were also lower in the PJ+ROT group ($p < 0.05$). The values correspond to an average of several measurements, specific to each time the PJ was freshly prepared. These results may suggest a decrease in functional mobility and increase motor impairment.

## 4. DISCUSSION

Several studies have demonstrated the efficacy of different types of polyphenols to attenuate or block neuronal death in animal models of neurodegeneration (Hartman et al., 2006; Maher et al., 2011; Ramassamy, 2006). Due to their broad pharmacological effects and therapeutic properties – including both antioxidant and anti-inflammatory actions – polyphenol compounds are now being considered for clinical trials in neurodegenerative disorders, such as PD. Given that DA neurons are highly susceptible to oxidative injury and inflammation, we hypothesized that treatment with PJ (rich in polyphenol content) in a progressive PD model using rotenone might confer neuroprotection. Contrary to our expectation, PJ failed to provide neuroprotection resulting in an exacerbation of rotenone-induced nigrostriatal degeneration.

Phytochemical compounds have been reported to be quite protective in the 6-OHDA and MPTP models of PD. Specifically, Yu and colleagues treated C57BL/6N mice with MPTP for 5 days, followed by curcumin (50 mg/kg i.p.) for 7 days (Yu et al., 2010). In parkinsonian rats, Zbarsky et al. used 4 different phytochemicals: curcumin and naringenin administered p.o. at 50 mg/kg dose and quercitin and fisetin administered p.o. at 20 mg/kg. On day 4 of treatment, one hour after the final dose of polyphenol, animals received a single unilateral injection of 6-OHDA and were sacrificed 7 days later. Only curcumin and naringenin provided neuroprotection (Zbarsky et al., 2005).

The reasons for this discrepancy between our results and previous studies are not known. Nonetheless, a crucial difference between our present work and the aforementioned studies is the use of a polyphenol mixture (PJ contains phenolic acids such as ellagic acid and gallic acid and flavonoids such as hydrolysable tannins [ellagitannins, gallotannins, punicalagin] and anthocyanins and their glycosides [pelargonidin, cyaniding, delphinidin]) instead of individual phytochemicals at high concentrations. An additional explanation may be the fundamental difference in the nature of the toxic insult between rotenone and the other neurotoxins. Rotenone is a pesticide, which crosses biological membranes quickly and without the need for transporters due to its lipophilic nature (Betarbet et al., 2000). Chronic administration of rotenone at low doses kills neurons primarily via oxidative mechanisms rather than by ATP depletion (Hensley et al., 1998; Sherer et al., 2003b). This occurs for two reasons: first, it is well established that complex I enzymatic activity must be inhibited quite substantially (typically > 60–70%) before there is a significant impact on ATP production (Davey and Clark, 1996; Greenamyre et al., 2001). Second, there is an electron leakage site upstream of the rotenone binding site in complex I, and when rotenone inhibits electron transfer, electrons can leak from complex I and then combine with molecular oxygen to form ROS (Hensley et al., 1998). Further, rotenone inhibits complex I uniformly in all cell types, including glia, while 6-OHDA and MPTP only affect the subset of neurons that express plasma membrane catecholamine transporters (Van Kampen et al., 2000). In addition, rotenone causes persistent inhibition of complex I – and concomitant oxidative stress – for the relatively extended duration of the experimental treatment (Betarbet et al., 2000).

Although differences between PD models could explain a lack of beneficial efficacy of PJ in the rotenone model, the question remains as to why PJ would exacerbate rotenone toxicity – similarly to melatonin (Tapias et al., 2010). A possible answer could be related to misconceptions about the antioxidant properties of PJ; polyphenolic phytochemicals are considered double-edged swords in cellular redox status. Experimental evidence in cell models supports the pro-oxidant nature of a large number of polyphenol compounds (Bouayed and Bohn, 2010; De Marchi et al., 2009; Elbling et al., 2005; Fukumoto and Mazza, 2000; Metodiewa et al., 1999). Polyphenols may lead to an increase of lipid peroxidation, DNA damage, mitochondrial damage, and caspase-3 activation, as well as intracellular glutathione depletion and ROS scavenging enzyme inhibition (Babich et al., 2007; Bhat et al., 2007; Chai et al., 2003; Galati and O'Brien, 2004; Raza and John, 2005; Watjen et al., 2005).

The balance between the beneficial and deleterious properties of polyphenols may be determined by a combination of the specific chemical administered and its dosage. In this regard, three different concentration-dependent cellular responses have been described: low doses induce mild oxidative stress; moderate exposure progressively overwhelms endogenous antioxidant systems and induces apoptosis; and high doses rapidly overwhelm the antioxidant defenses and induce oxidative damage, leading to necrosis (Babich et al., 2011). Likewise, polyphenol compounds can exhibit pro-oxidant properties in the presence of transition metal ions. Epigallocatechin gallate (EGCG) acts to reduce $Fe^{3+}$ to $Fe^{2+}$, which promotes hydroxyl radical formation via the chemical Fenton reaction; it has been suggested that EGCG toxicity is due to its capacity to generate hydrogen peroxide that is predominantly $Fe^{2+}$-dependent (Nakagawa et al., 2004). Polyphenolic compounds can also catalyze DNA degradation in the presence of copper; the postulated mechanism is that polyphenols (i) can directly interact with $Cu^{2+}$ (Oikawa et al., 2003) or (ii) can bind to DNA and $Cu^{2+}$ to form a ternary complex (Bhat et al., 2007). During the process, $Cu^{2+}$ is reduced to $Cu^{+}$, which interacts with the hydrogen peroxide to produce hydroxyl radicals through the Fenton reaction.

It has been reported that exogenous treatment with antioxidants such as N-acetyl cysteine and reduced glutathione considerably reduced the pro-oxidant effects of polyphenols (Fujisawa et al., 2004), supporting the notion that the cytotoxicity may be hydrogen peroxide and superoxide anion dependent (Vittal et al., 2004; Yen et al., 2004). These compounds can also elicit transcriptional changes mediated by NF-E2-related factor 2 binding to antioxidant response elements (Crespo et al., 2010; Romeo et al., 2009).

Significant evidence in support of polyphenolic pro-oxidant properties has been similarly demonstrated in animal models. EGCG collapsed mitochondrial membrane potential and induced ROS production in a time and dose-dependent manner in mouse hepatocytes (Galati et al., 2006). Toxic urinary metabolites were identified following i.p. injections of high doses of EGCG to mice; these metabolites are hypothesized to arise from the reaction of EGCG quinone intermediates with the thiol group of cysteine in the presence of glutathione (Sang et al., 2005). Oral administration of EGCG caused hepatotoxicity in mice that was associated with enhanced lipid peroxidation and γ-histone 2AX expression (Lambert et al., 2010).

In essence, pro-oxidant effects of PJ (or melatonin) may elicit a “preconditioning” or “postconditioning” protective response mediated by endogenous antioxidant response machinery. We suggest that initial oxidative stress might be scavenged or mitigated by the antioxidant capability of PJ; however, when there is substantial ongoing oxidative stress – as in the rotenone model and presumably, PD – the antioxidant response wanes or is

overwhelmed over time, and at that point, the pro-oxidant effects predominate and PJ could potentially act as a pro-oxidant.

Detrimental effects of polyphenolic compounds may also occur as a result of the initiation of specific cellular processes, including inflammatory signaling pathways. In PD, impairment of complex I leads to accumulation of NADH and the redox potential of the matrix becomes low, resulting in an excessive ROS and RNS production and microglial activation. Dopamine neurons are inherently susceptible to the deleterious effect of reactive microglia because these inflammatory cells are a major source of free radicals that may impair macromolecules (Block and Hong, 2005). In addition, DA neurons are particularly sensitive to oxidative stress due to their low antioxidant capacity, as evidenced by low intracellular glutathione (Sian et al., 1994). Additionally a proinflammatory effect of polyphenols *in vivo* has been shown, which may involve modulation of the migration and function of T cells (Graff and Jutila, 2007).

To test the hypothesis that PJ can become a pro-oxidant, both oxidative and nitrosative stress were examined in the SN of rats. Evidence from postmortem parkinsonian brain tissue suggests that ROS and RNS are important contributors to the nigral DA neuron degeneration (Danielson and Andersen, 2008; Giasson et al., 2002). Nitric oxide ($NO^{\bullet}$), which when oxidized produces RNS, could be the primary agent involved in preferential complex I inhibition in DA neurons in PD and may cause protein alterations. Increased NT immunoreactivity has been detected in the SN of PD patients (Good et al., 1998). Furthermore, the process of lipid peroxidation yields several major products, including 4-HNE and malondialdehyde (MDA) which are considered to be biomarkers of oxidative stress (Esterbauer et al., 1991). Human studies indicate an accumulation of 4-HNE and MDA in the SN of parkinsonian patients (Dexter et al., 1989; Yoritaka et al., 1996).

A large body of evidence also supports the involvement of inflammation in PD, and is generally typified by an accumulation of activated microglia (Wu et al., 2002). Upon activation of microglia, expression of Iba1 is upregulated. Microglial activation also causes $NO^{\bullet}$ overproduction via iNOS induction (Liberatore et al., 1999). Examination of postmortem PD brains has revealed robust microgliosis (McGeer et al., 1988) and the presence of high levels of iNOS expression in the SN compared to age-matched controls (Knott et al., 2000). Proinflammatory cytokines such as IL-1β and TNF-α, enzymes such as iNOS and COX-2, and transcription factors such as NF-kB – a pleiotropic redox-sensitive transcriptional factor that can modulate the expression of a plethora of genes – appear to be involved in DA toxicity and have been observed in cerebrospinal fluid and postmorten brain tissue of parkinsonian patients (Boka et al., 1994; Hunot et al., 1997; Knott et al., 2000; Mogi et al., 1996; Teismann et al., 2003).

Rotenone induces oxidative stress in rats and its chronic administration increased $NO^{\bullet}$ and lipid peroxidation in rat cortical and nigrostriatal regions (Bashkatova et al., 2004; He et al., 2003). Moreover, chronic treatment of rotenone increases both iNOS enzymatic activity and mRNA levels (Yang et al., 2005) and provokes selective nigrostriatal microglial activation in rats (Sherer et al., 2003a).

The present findings showed robust nigrostriatal damage and increased NT, 4-HNE, iNOS, Iba1, and activated caspase-3 expression in response to rotenone. Importantly, administration of PJ alone increased nitrosative stress, iNOS immunoreactivity, and cleaved caspase-3, suggesting a role of $NO^{\bullet}$ in PJ-induced degeneration of nigral DA neurons. Following rotenone exposure, oral administration of PJ worsened behavior, enhanced nitrosative stress, increased iNOS and NF-kB expression, and induced caspase-3 activation, heightening rotenone toxicity. In addition, co-administration of PJ and rotenone decreased

striatal TH immunoreactivity and induced SN neuron loss relative to rats treated with rotenone alone; however, no difference in monoamine content was observed. This "paradoxical" finding may be explained by reports indicating that in partial denervation of the nigrostriatal DA system, surviving DA terminals are able to maintain DA content despite moderate DA cell loss (Abercrombie et al., 1990; Cohen et al., 2011; Robinson et al., 1994).

In summary, our data provide novel, strong evidence for a pro-oxidant effect of PJ in a PD model and provide insight into the mechanism by which this may occur. Moreover, our results suggest that further careful investigation into the effects of PJ in neurodegeneration is necessary.

## Supplementary Material

Refer to Web version on PubMed Central for supplementary material.

## Acknowledgments

This work was supported by NIH grants NS059806 and ES018058 and the American Parkinson Disease Association (J.T.G), the Fulbright Commission, Ministry of Education and Science, Madrid, Spain (Fulbright Fellowship to V.T.), and NIH grant ES019879 (J.R.C). We especially thank Theresa Hayden, Tony Balko and Laura Montero for their contributions and Terina Martinez for early draft editing.

## REFERENCES

Abercrombie ED, et al. Effects of L-dopa on extracellular dopamine in striatum of normal and 6-hydroxydopamine-treated rats. Brain Res. 1990; 525:36–44. [PubMed: 2123121]

Aviram M, et al. Pomegranate phenolics from the peels, arils, and flowers are antiatherogenic: studies in vivo in atherosclerotic apolipoprotein e-deficient (E 0) mice and in vitro in cultured macrophages and lipoproteins. J Agric Food Chem. 2008; 56:1148–1157. [PubMed: 18173244]

Babich H, et al. Research strategies in the study of the pro-oxidant nature of polyphenol nutraceuticals. J Toxicol. 2011; 2011:467305. [PubMed: 21776260]

Babich H, et al. Glutathione as a mediator of the in vitro cytotoxicity of a green tea polyphenol extract. Toxicol Mech Methods. 2007; 17:357–369. [PubMed: 20020959]

Bashkatova V, et al. Chronic administration of rotenone increases levels of nitric oxide and lipid peroxidation products in rat brain. Exp Neurol. 2004; 186:235–241. [PubMed: 15026259]

Beal MF. Mitochondria take center stage in aging and neurodegeneration. Ann Neurol. 2005; 58:495–505. [PubMed: 16178023]

Beckman JS, et al. Apparent hydroxyl radical production by peroxynitrite: implications for endothelial injury from nitric oxide and superoxide. Proc Natl Acad Sci U S A. 1990; 87:1620–1624. [PubMed: 2154753]

Betarbet R, et al. Chronic systemic pesticide exposure reproduces features of Parkinson's disease. Nat Neurosci. 2000; 3:1301–1306. [PubMed: 11100151]

Bhat SH, et al. Prooxidant DNA breakage induced by caffeic acid in human peripheral lymphocytes: involvement of endogenous copper and a putative mechanism for anticancer properties. Toxicol Appl Pharmacol. 2007; 218:249–255. [PubMed: 17208261]

Block ML, Hong JS. Microglia and inflammation-mediated neurodegeneration: multiple triggers with a common mechanism. Prog Neurobiol. 2005; 76:77–98. [PubMed: 16081203]

Boka G, et al. Immunocytochemical analysis of tumor necrosis factor and its receptors in Parkinson's disease. Neurosci Lett. 1994; 172:151–154. [PubMed: 8084523]

Bouayed J, Bohn T. Exogenous antioxidants - Double-edged swords in cellular redox state: Health beneficial effects at physiologic doses versus deleterious effects at high doses. Oxid Med Cell Longev. 2010; 3:228–237. [PubMed: 20972369]

Cadet JL, Brannock C. Free radicals and the pathobiology of brain dopamine systems. Neurochem Int. 1998; 32:117–131. [PubMed: 9542724]

Cannon JR, et al. A highly reproducible rotenone model of Parkinson's disease. Neurobiol Dis. 2009; 34:279–290. [PubMed: 19385059]

Chai PC, et al. Contribution of hydrogen peroxide to the cytotoxicity of green tea and red wines. Biochem Biophys Res Commun. 2003; 304:650–654. [PubMed: 12727203]

Chinta SJ, et al. Inducible alterations of glutathione levels in adult dopaminergic midbrain neurons result in nigrostriatal degeneration. J Neurosci. 2007; 27:13997–14006. [PubMed: 18094238]

Cohen AD, et al. Effects of intrastriatal GDNF on the response of dopamine neurons to 6-hydroxydopamine: time course of protection and neurorestoration. Brain Res. 2011; 1370:80–88. [PubMed: 21062624]

Crespo I, et al. Melatonin prevents the decreased activity of antioxidant enzymes and activates nuclear erythroid 2-related factor 2 signaling in an animal model of fulminant hepatic failure of viral origin. J Pineal Res. 2010; 49:193–200. [PubMed: 20609075]

Danielson SR, Andersen JK. Oxidative and nitrative protein modifications in Parkinson's disease. Free Radic Biol Med. 2008; 44:1787–1794. [PubMed: 18395015]

Davey GP, Clark JB. Threshold effects and control of oxidative phosphorylation in nonsynaptic rat brain mitochondria. J Neurochem. 1996; 66:1617–1624. [PubMed: 8627318]

De Marchi U, et al. Quercetin can act either as an inhibitor or an inducer of the mitochondrial permeability transition pore: A demonstration of the ambivalent redox character of polyphenols. Biochim Biophys Acta. 2009; 1787:1425–1432. [PubMed: 19523917]

Dexter DT, et al. Basal lipid peroxidation in substantia nigra is increased in Parkinson's disease. J Neurochem. 1989; 52:381–389. [PubMed: 2911023]

Elbling L, et al. Green tea extract and (−)-epigallocatechin-3-gallate, the major tea catechin, exert oxidant but lack antioxidant activities. FASEB J. 2005; 19:807–809. [PubMed: 15738004]

Esterbauer H, et al. Chemistry and biochemistry of 4-hydroxynonenal, malonaldehyde and related aldehydes. Free Radic Biol Med. 1991; 11:81–128. [PubMed: 1937131]

Fujisawa S, et al. Cytotoxicity, ROS-generation activity and radical-scavenging activity of curcumin and related compounds. Anticancer Res. 2004; 24:563–569. [PubMed: 15160995]

Fukumoto LR, Mazza G. Assessing antioxidant and prooxidant activities of phenolic compounds. J Agric Food Chem. 2000; 48:3597–3604. [PubMed: 10956156]

Galati G, et al. Cellular and in vivo hepatotoxicity caused by green tea phenolic acids and catechins. Free Radic Biol Med. 2006; 40:570–580. [PubMed: 16458187]

Galati G, O'Brien PJ. Potential toxicity of flavonoids and other dietary phenolics: significance for their chemopreventive and anticancer properties. Free Radic Biol Med. 2004; 37:287–303. [PubMed: 15223063]

Giasson BI, et al. The relationship between oxidative/nitrative stress and pathological inclusions in Alzheimer's and Parkinson's diseases. Free Radic Biol Med. 2002; 32:1264–1275. [PubMed: 12057764]

Gil MI, et al. Antioxidant activity of pomegranate juice and its relationship with phenolic composition and processing. J Agric Food Chem. 2000; 48:4581–4589. [PubMed: 11052704]

Good PF, et al. Protein nitration in Parkinson's disease. J Neuropathol Exp Neurol. 1998; 57:338–342. [PubMed: 9600227]

Graff JC, Jutila MA. Differential regulation of CD11b on gammadelta T cells and monocytes in response to unripe apple polyphenols. J Leukoc Biol. 2007; 82:603–607. [PubMed: 17540733]

Greenamyre JT, et al. Complex I and Parkinson's disease. IUBMB Life. 2001; 52:135–141. [PubMed: 11798025]

Guo S, et al. Protective effects of green tea polyphenols in the 6-OHDA rat model of Parkinson's disease through inhibition of ROS-NO pathway. Biol Psychiatry. 2007; 62:1353–1362. [PubMed: 17624318]

Hartman RE, et al. Pomegranate juice decreases amyloid load and improves behavior in a mouse model of Alzheimer's disease. Neurobiol Dis. 2006; 24:506–515. [PubMed: 17010630]

He Y, et al. Role of nitric oxide in rotenone-induced nigro-striatal injury. J Neurochem. 2003; 86:1338–1345. [PubMed: 12950443]

Hensley K, et al. Interaction of alpha-phenyl-N-tert-butyl nitrone and alternative electron acceptors with complex I indicates a substrate reduction site upstream from the rotenone binding site. J Neurochem. 1998; 71:2549–2557. [PubMed: 9832155]

Hu LF, et al. Neuroprotective effects of hydrogen sulfide on Parkinson's disease rat models. Aging Cell. 2010; 9:135–146. [PubMed: 20041858]

Hunot S, et al. Nuclear translocation of NF-kappaB is increased in dopaminergic neurons of patients with parkinson disease. Proc Natl Acad Sci U S A. 1997; 94:7531–7536. [PubMed: 9207126]

Jenner P. Oxidative stress in Parkinson's disease. Ann Neurol. 2003; 53(Suppl 3):S26–S36. discussion S36-28. [PubMed: 12666096]

Knott C, et al. Inflammatory regulators in Parkinson's disease: iNOS, lipocortin-1, and cyclooxygenases-1 and-2. Mol Cell Neurosci. 2000; 16:724–739. [PubMed: 11124893]

Koyama S, et al. Pomegranate extract induces apoptosis in human prostate cancer cells by modulation of the IGF-IGFBP axis. Growth Horm IGF Res. 2010; 20:55–62. [PubMed: 19853487]

Lambert JD, et al. Hepatotoxicity of high oral dose (−)-epigallocatechin-3-gallate in mice. Food Chem Toxicol. 2010; 48:409–416. [PubMed: 19883714]

Levites Y, et al. Attenuation of 6-hydroxydopamine (6-OHDA)-induced nuclear factorkappaB (NF-kappaB) activation and cell death by tea extracts in neuronal cultures. Biochem Pharmacol. 2002; 63:21–29. [PubMed: 11754870]

Liang LP, et al. An orally active catalytic metalloporphyrin protects against 1-methyl-4-phenyl-1,2,3,6-tetrahydropyridine neurotoxicity in vivo. J Neurosci. 2007; 27:4326–4333. [PubMed: 17442816]

Liberatore GT, et al. Inducible nitric oxide synthase stimulates dopaminergic neurodegeneration in the MPTP model of Parkinson disease. Nat Med. 1999; 5:1403–1409. [PubMed: 10581083]

Maher P, et al. ERK activation by the polyphenols fisetin and resveratrol provides neuroprotection in multiple models of Huntington's disease. Hum Mol Genet. 2011; 20:261–270. [PubMed: 20952447]

McGeer PL, et al. Reactive microglia are positive for HLA-DR in the substantia nigra of Parkinson's and Alzheimer's disease brains. Neurology. 1988; 38:1285–1291. [PubMed: 3399080]

Metodiewa D, et al. Quercetin may act as a cytotoxic prooxidant after its metabolic activation to semiquinone and quinoidal product. Free Radic Biol Med. 1999; 26:107–116. [PubMed: 9890646]

Mogi M, et al. Interleukin (IL)-1 beta, IL-2, IL-4, IL-6 and transforming growth factoralpha levels are elevated in ventricular cerebrospinal fluid in juvenile parkinsonism and Parkinson's disease. Neurosci Lett. 1996; 211:13–16. [PubMed: 8809836]

Nakagawa H, et al. Generation of hydrogen peroxide primarily contributes to the induction of Fe(II)-dependent apoptosis in Jurkat cells by (−)-epigallocatechin gallate. Carcinogenesis. 2004; 25:1567–1574. [PubMed: 15090467]

Oikawa S, et al. Catechins induce oxidative damage to cellular and isolated DNA through the generation of reactive oxygen species. Free Radic Res. 2003; 37:881–890. [PubMed: 14567448]

Ramassamy C. Emerging role of polyphenolic compounds in the treatment of neurodegenerative diseases: a review of their intracellular targets. Eur J Pharmacol. 2006; 545:51–64. [PubMed: 16904103]

Raza H, John A. Green tea polyphenol epigallocatechin-3-gallate differentially modulates oxidative stress in PC12 cell compartments. Toxicol Appl Pharmacol. 2005; 207:212–220. [PubMed: 16129114]

Robinson TE, et al. Time course of recovery of extracellular dopamine following partial damage to the nigrostriatal dopamine system. J Neurosci. 1994; 14:2687–2696. [PubMed: 7514209]

Romeo L, et al. The major green tea polyphenol, (−)-epigallocatechin-3-gallate, induces heme oxygenase in rat neurons and acts as an effective neuroprotective agent against oxidative stress. J Am Coll Nutr. 2009; (28 Suppl):492S–499S. [PubMed: 20234037]

Sang S, et al. Synthesis and structure identification of thiol conjugates of (−)-epigallocatechin gallate and their urinary levels in mice. Chem Res Toxicol. 2005; 18:1762–1769. [PubMed: 16300386]

Schallert, T.; Tillerson, JL. Intervention strategies for degeneration of dopamine neurons in parkinsonism: optimizing behavioral assessment of outcome. In: Emerich DF, DRI.; Sanberg, PR.,

editors. Central Nervous System Diseases: Innovative models of CNS diseases from molecule to therapy. Totowa, New Jersey, United States: Humana Press; 2000. p. 131-151.

Schapira AH, et al. Mitochondrial complex I deficiency in Parkinson's disease. Lancet. 1989; 1:1269. [PubMed: 2566813]

Sherer TB, et al. Selective microglial activation in the rat rotenone model of Parkinson's disease. Neurosci Lett. 2003a; 341:87–90. [PubMed: 12686372]

Sherer TB, et al. Mechanism of toxicity in rotenone models of Parkinson's disease. J Neurosci. 2003b; 23:10756–10764. [PubMed: 14645467]

Sian J, et al. Alterations in glutathione levels in Parkinson's disease and other neurodegenerative disorders affecting basal ganglia. Ann Neurol. 1994; 36:348–355. [PubMed: 8080242]

Tapias V, et al. Melatonin treatment potentiates neurodegeneration in a rat rotenone Parkinson's disease model. J Neurosci Res. 2010; 88:420–427. [PubMed: 19681169]

Tapias V, et al. Melatonin and its brain metabolite N(1)-acetyl-5-methoxykynuramine prevent mitochondrial nitric oxide synthase induction in parkinsonian mice. J Neurosci Res. 2009; 87:3002–3010. [PubMed: 19437546]

Tapias V, et al. Automated imaging system for fast quantitation of neurons, cell morphology and neurite morphometry in vivo and in vitro. Neurobiol Dis. 2012

Teismann P, et al. Cyclooxygenase-2 is instrumental in Parkinson's disease neurodegeneration. Proc Natl Acad Sci U S A. 2003; 100:5473–5478. [PubMed: 12702778]

Van Kampen JM, et al. Dopamine transporter function assessed by antisense knockdown in the rat: protection from dopamine neurotoxicity. Synapse. 2000; 37:171–178. [PubMed: 10881039]

Vittal R, et al. Gene expression changes induced by green tea polyphenol (−)-epigallocatechin-3-gallate in human bronchial epithelial 21BES cells analyzed by DNA microarray. Mol Cancer Ther. 2004; 3:1091–1099. [PubMed: 15367703]

Watjen W, et al. Low concentrations of flavonoids are protective in rat H4IIE cells whereas high concentrations cause DNA damage and apoptosis. J Nutr. 2005; 135:525–531. [PubMed: 15735088]

Woodlee MT, et al. Enhanced function in the good forelimb of hemi-parkinson rats: compensatory adaptation for contralateral postural instability? Exp Neurol. 2008; 211:511–517. [PubMed: 18417125]

Wu DC, et al. Blockade of microglial activation is neuroprotective in the 1-methyl-4-phenyl-1,2,3,6-tetrahydropyridine mouse model of Parkinson disease. J Neurosci. 2002; 22:1763–1771. [PubMed: 11880505]

Wu HM, et al. Novel neuroprotective mechanisms of memantine: increase in neurotrophic factor release from astroglia and anti-inflammation by preventing microglial activation. Neuropsychopharmacology. 2009; 34:2344–2357. [PubMed: 19536110]

Yang Y, et al. Systematic administration of iptakalim, an ATP-sensitive potassium channel opener, prevents rotenone-induced motor and neurochemical alterations in rats. J Neurosci Res. 2005; 80:442–449. [PubMed: 15795934]

Yen GC, et al. Modulation of tea and tea polyphenols on benzo(a)pyrene-induced DNA damage in Chang liver cells. Free Radic Res. 2004; 38:193–200. [PubMed: 15104213]

Yoritaka A, et al. Immunohistochemical detection of 4-hydroxynonenal protein adducts in Parkinson disease. Proc Natl Acad Sci U S A. 1996; 93:2696–2701. [PubMed: 8610103]

Yu S, et al. Curcumin prevents dopaminergic neuronal death through inhibition of the c-Jun N-terminal kinase pathway. Rejuvenation Res. 2010; 13:55–64. [PubMed: 20230279]

Zbarsky V, et al. Neuroprotective properties of the natural phenolic antioxidants curcumin and naringenin but not quercetin and fisetin in a 6-OHDA model of Parkinson's disease. Free Radic Res. 2005; 39:1119–1125. [PubMed: 16298737]

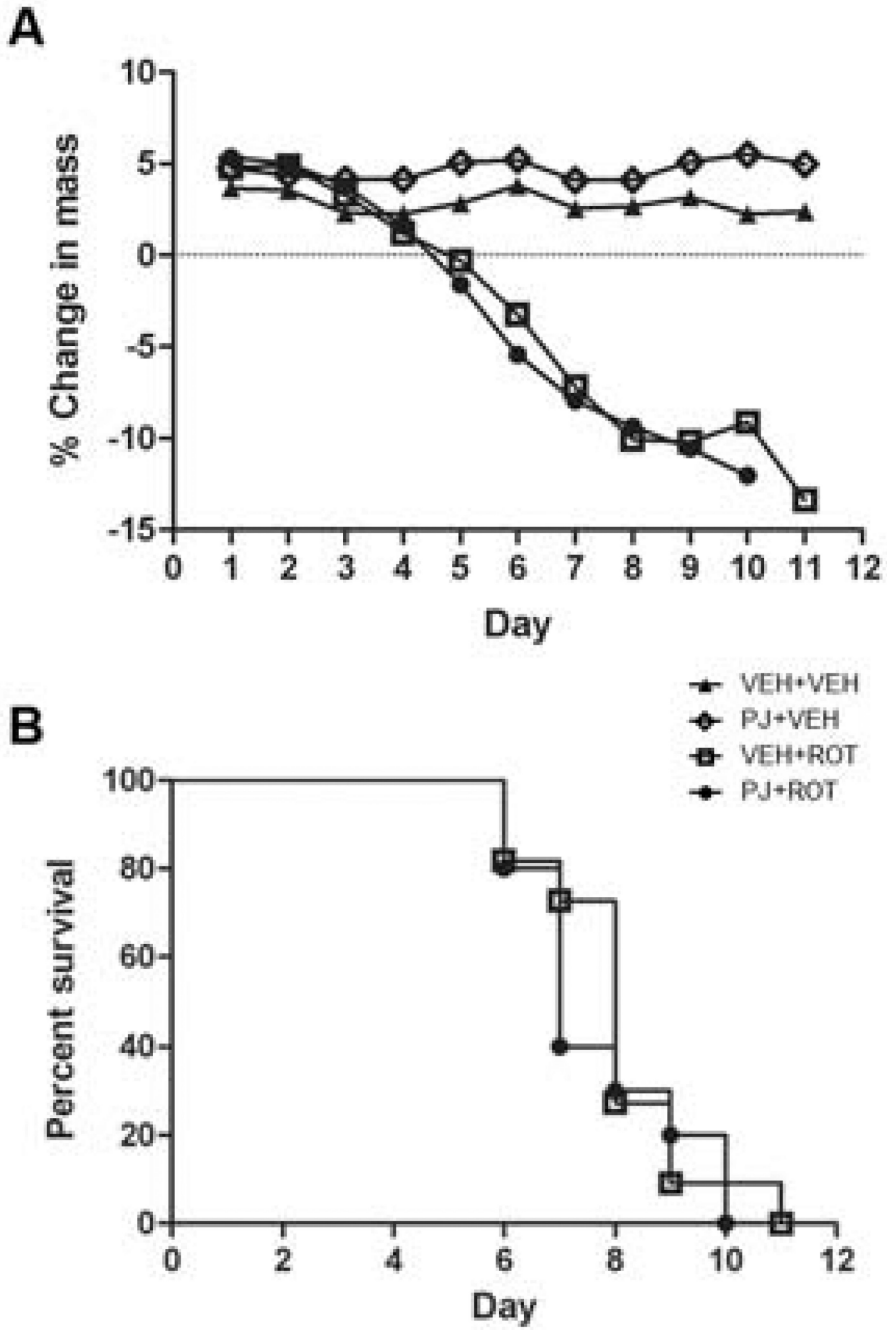


**Figure 1.**

Dietary treatment with PJ does not attenuate weight loss or prevent development of a parkinsonian phenotype in the rotenone model. ***(A)*** The percent change in body mass, relative to mass at the onset of treatment (day 0) with rotenone (3.0 mg/kg/day), PJ (~7 mL/day) or vehicle. Note that the percent mass change is relatively similar for both groups (VEH+ROT and PJ+ROT) at all-time points. ***(B)*** Survival curves following rotenone administration. Rats were euthanized when they developed a debilitating PD phenotype, as characterized by severe bradykinesia, rigidity, and postural instability. No difference in

overall survival was observed between the VEH+ROT group (empty squares) and the PJ +ROT group (filled circles).

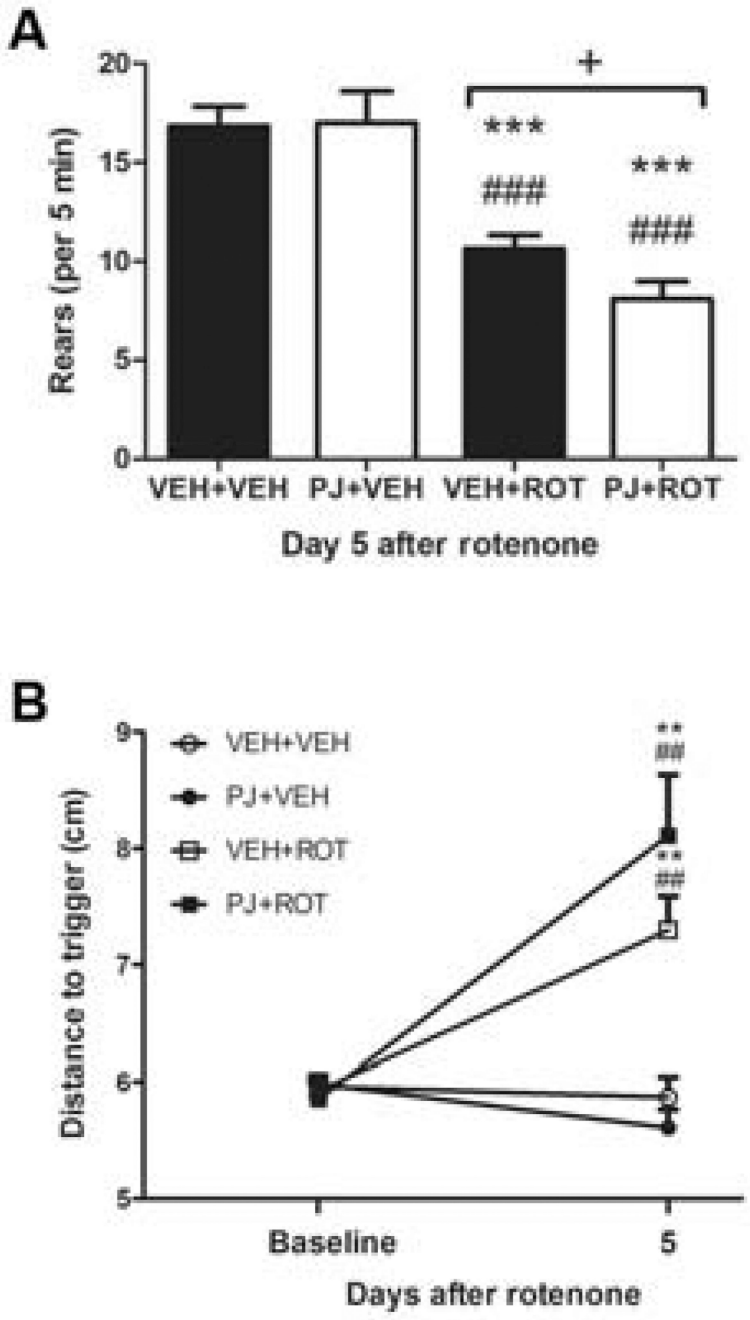


**Figure 2.**

Neurobehavioral assessment. ***(A)*** After 5 days of rotenone treatment, rearing activity was observed over a 5 min period and scored for each group. *** $p < 0.001$ compared to VEH +VEH, Newman-Keuls post-hoc test; ### $p < 0.001$ vs PJ+VEH; + $p < 0.05$ vs VEH+ROT. ***(B)*** Postural instability at baseline, prior to administration of rotenone, and 5 days after rotenone administration (two way-ANOVA, ** $p < 0.01$ vs VEH+VEH; ## $p < 0.01$ vs PJ +VEH). For all tests, n = 6 for control and n = 11 for rotenone-treated.

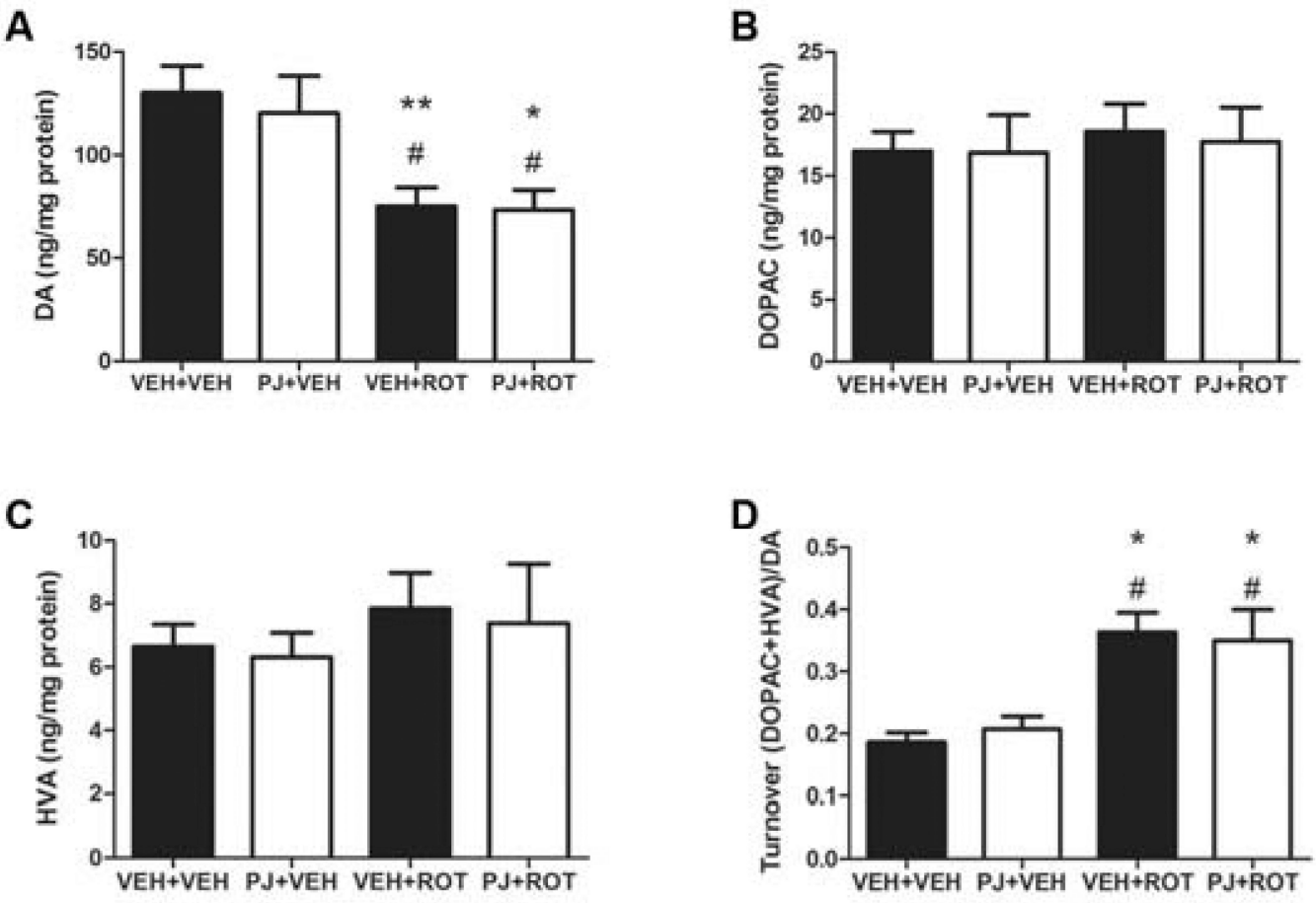


**Figure 3.**

Striatal catecholamine levels and turnover. DA (***A***), DOPAC (***B***), HVA (***C***), and DA turnover (DOPAC+HVA)/DA) (***D***). Rotenone induced a decrease in DA levels and turnover. Supplementation with PJ had no effect either alone or after neurotoxin exposure. Data are means ± S.E.M. ** $p < 0.01$, * $p < 0.05$ compared to VEH+VEH, Newman-Keuls post-hoc test; # $p < 0.05$ compared to PJ+VEH.

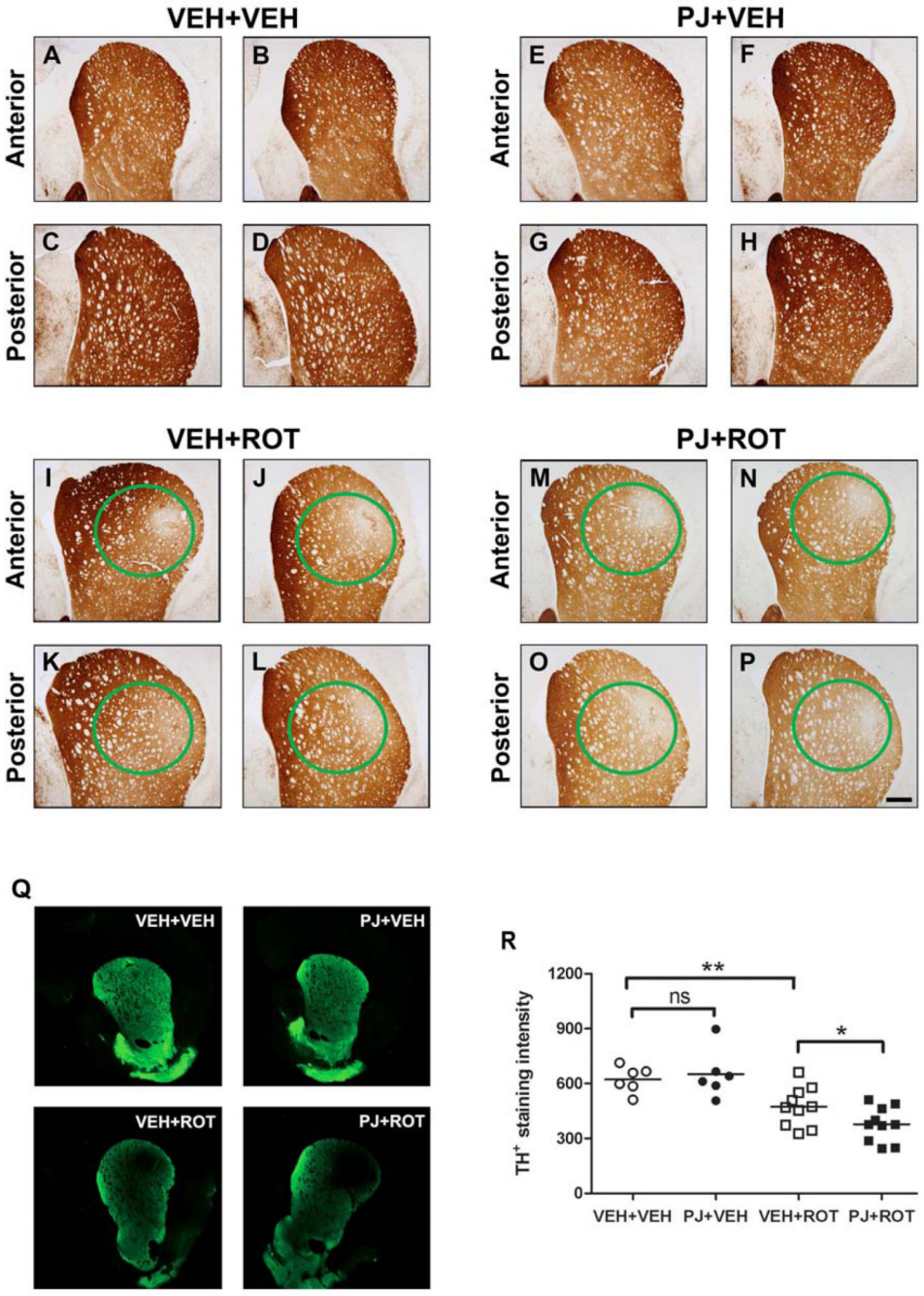


**Figure 4.**

Staining for tyrosine hydroxylase fiber loss in the striatum. Representative images of striatal TH immunohistochemistry from two animals in each group are shown. Rotenone led to degeneration of the DA terminals in the striatum, as evidenced by a focal loss of TH immunopositive fibers in anterior and posterior striatal sections (***I-L***) compared to control animals (***A-D***). Oral supplementation with PJ alone did not have any effect (***E-H***), but when administered together with rotenone, induced an overall decrease in striatal TH immunoreactivity (***M-P***). Green circles denote the area of the lesion. Note that the lesions are strikingly similar in magnitude and localization across animals. Scale bar = 500 μm.

Representative immunofluorescence-stained sections were depicted (***Q***) and quantified (***R***) with values representing average striatal intensity from three to five sections per animal. ** $p < 0.01$ vs VEH+VEH, Newman-Keuls post-hoc test; * $p < 0.05$ vs VEH+ROT.

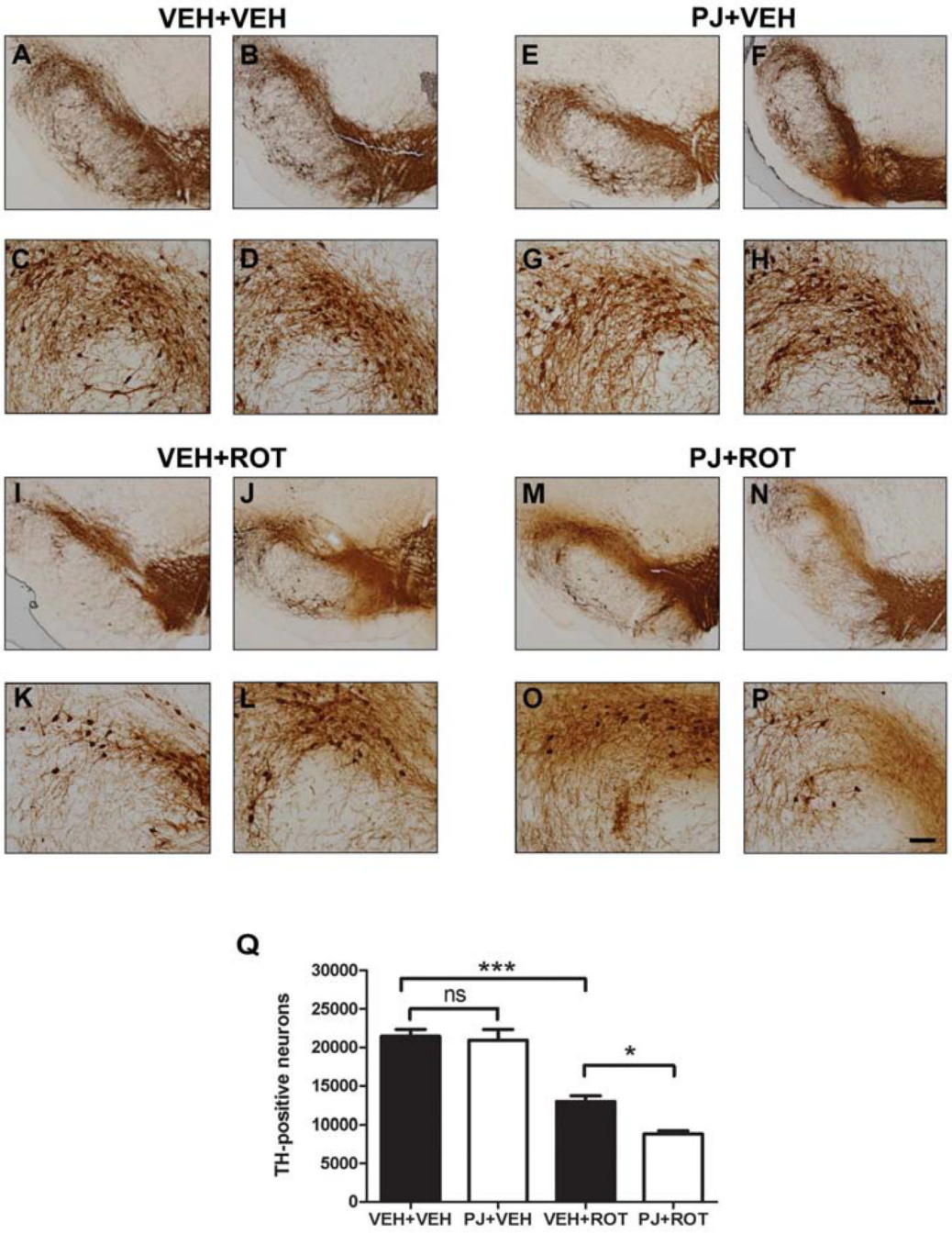


**Figure 5.**

Immunostaining of tyrosine hydroxylase-positive neurons in the substantia nigra. Examination at low (scale bar = 500 μm) and high magnification (scale bar = 50 μm) of the dorsolateral nigra revealed a dense TH-immunopositive network of cell bodies and fibers in the SN in controls alone (***A-D***) or with PJ (***E-H***). After the rotenone injections, there was a reduction in TH immunoreactivity at the level of the SN (***I-L***). Oral administration of PJ with rotenone caused an increase in DA cell loss and pruning of processes compared to treatment with rotenone alone (***M-P***). The loss of SN neurons was counted by unbiased stereology, and rats treated with PJ showed potentiation of rotenone-induced neurotoxicity

(***Q***). Bars represent means ± S.E.M. Statistical analyses were carried out using the Newman Keuls post-hoc test. *** $p < 0.001$ vs VEH+VEH; * $p < 0.05$ vs VEH+ROT.

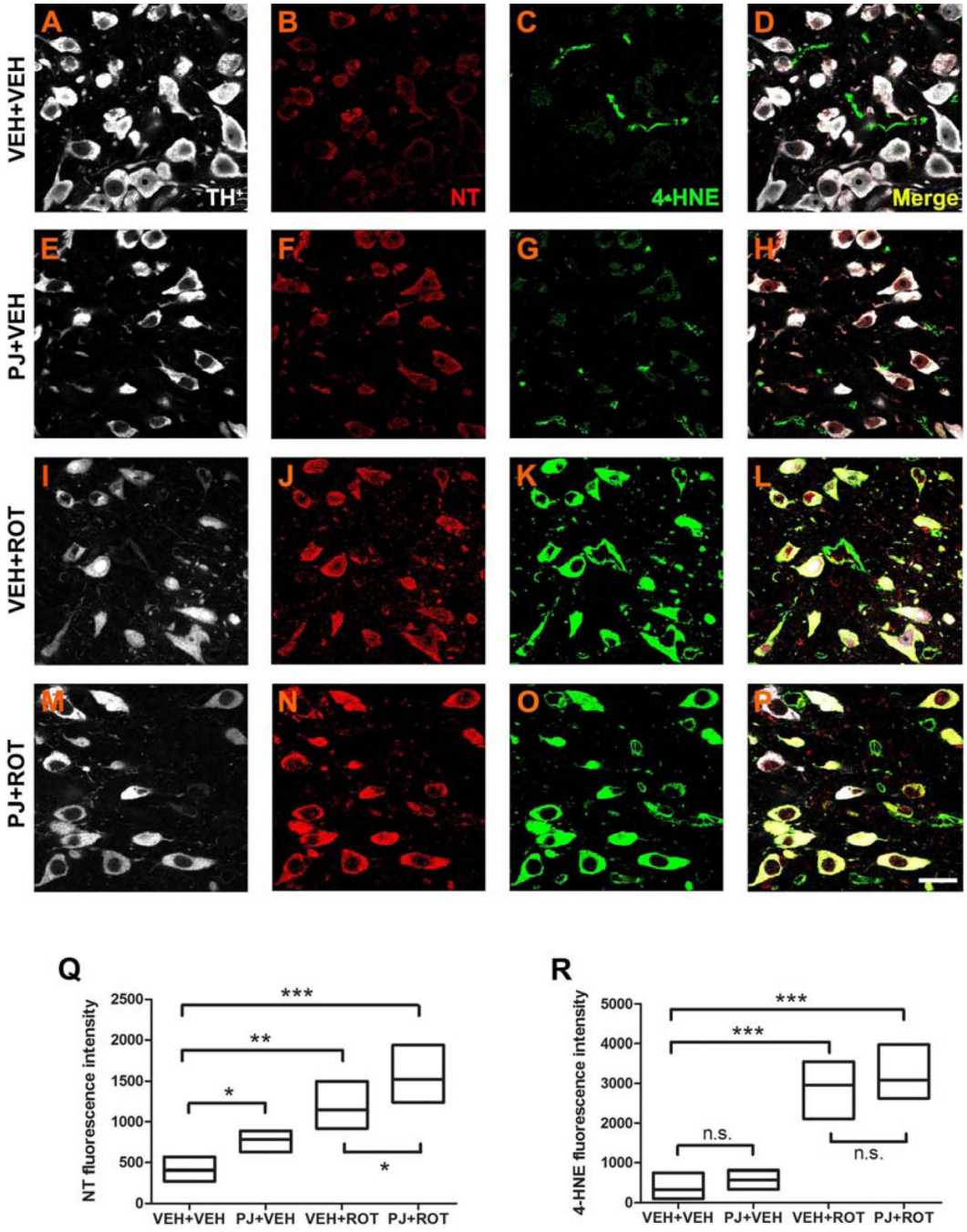


**Figure 6.**

Representative 100x confocal images for NT and 4-HNE immunostaining in SN sections. NT and 4-HNE were weakly expressed in controls (***B*** and ***C***). Increased expression of NT was noticed after oral treatment of PJ (***F***). Rotenone administration strongly enhanced NT immunoreactivity (***J***), which was further augmented when PJ was co-administered with the neurotoxin (***N***). A similar rotenone effect was observed for 4-HNE expression; however, PJ +ROT-treated animals did not exhibit significant differences relative to the rotenone-treated group (***O*** vs ***K***). White: $TH^+$; red: NT; green: 4-HNE. Quantification of the percentage of fluorescence intensity for NT levels (***Q***) and 4-HNE (***R***) was assessed, with data

representing average fluorescence immunoreactivity from 5 SN sections per animal (200–300 neurons per animal). Each treatment group was comprised of 4 rats. Scale bar = 20 μm. *** $p < 0.001$, ** $p < 0.01$, * $p < 0.05$ compared to VEH+VEH or VEH+ROT, Newman-Keuls post-hoc test.

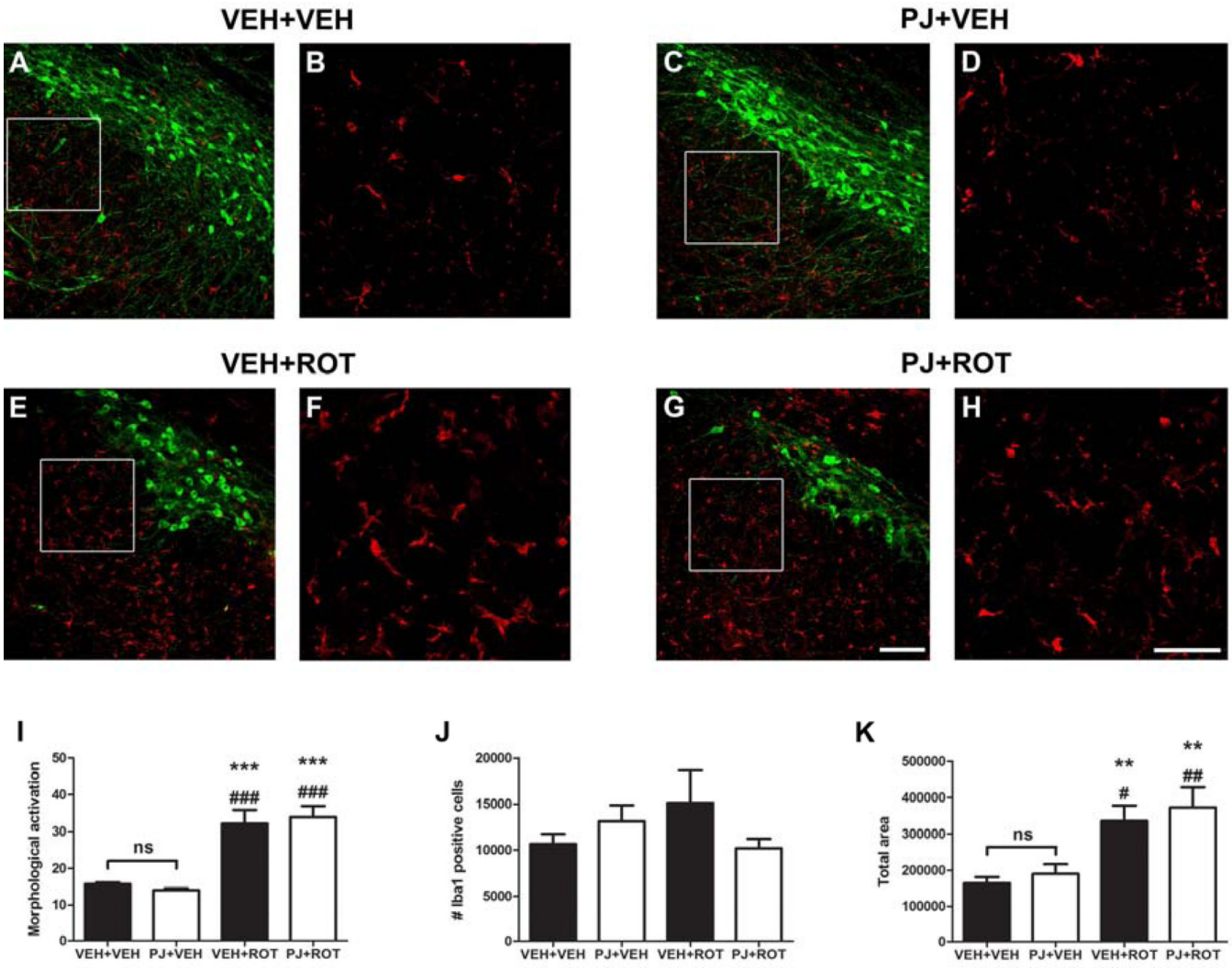


**Figure 7.**

Microscopy images of the immunohistochemistry for activated microglia. Immunofluorescence images of the entire SN were acquired. Untreated animals revealed a minimum expression of Iba1 (***A*** and inset ***B***) and oral administration of PJ did not alter Iba1 immunoreactivity (***C*** and inset ***D***). However, under pathological conditions, chronic rotenone treatment induced significant alterations in the morphology of nigral Iba1 positive cells (***E*** and inset ***F***). Iba1 expression remains unaltered after ROT+PJ treatment (***G*** and inset ***H***) relative to the rotenone-treated group. Quantitative analysis of Iba1 was carried out in 5 nigral sections and data is provided for "morphological activation" (***I***), number of Iba1 cells (***J***), and total area occupied by the microglial particles (***K***). Rotenone-induced toxicity caused a significant increase in the average size of Iba1 cells, but no changes were appreciated in the total number of cells. Oral administration of PJ did not induce microglial activation either by itself or combined with rotenone. Green: $TH^+$; red: Iba-1. Scale bar: 50 μm. The histogram values represent the mean ± S.E.M. Significant differences between groups were determined by Newman-Keuls post-hoc test. *** $p < 0.001$, ** $p < 0.01$ vs VEH+VEH. ### $p < 0.001$, ## $p < 0.01$, # $p < 0.05$ vs PJ+VEH.

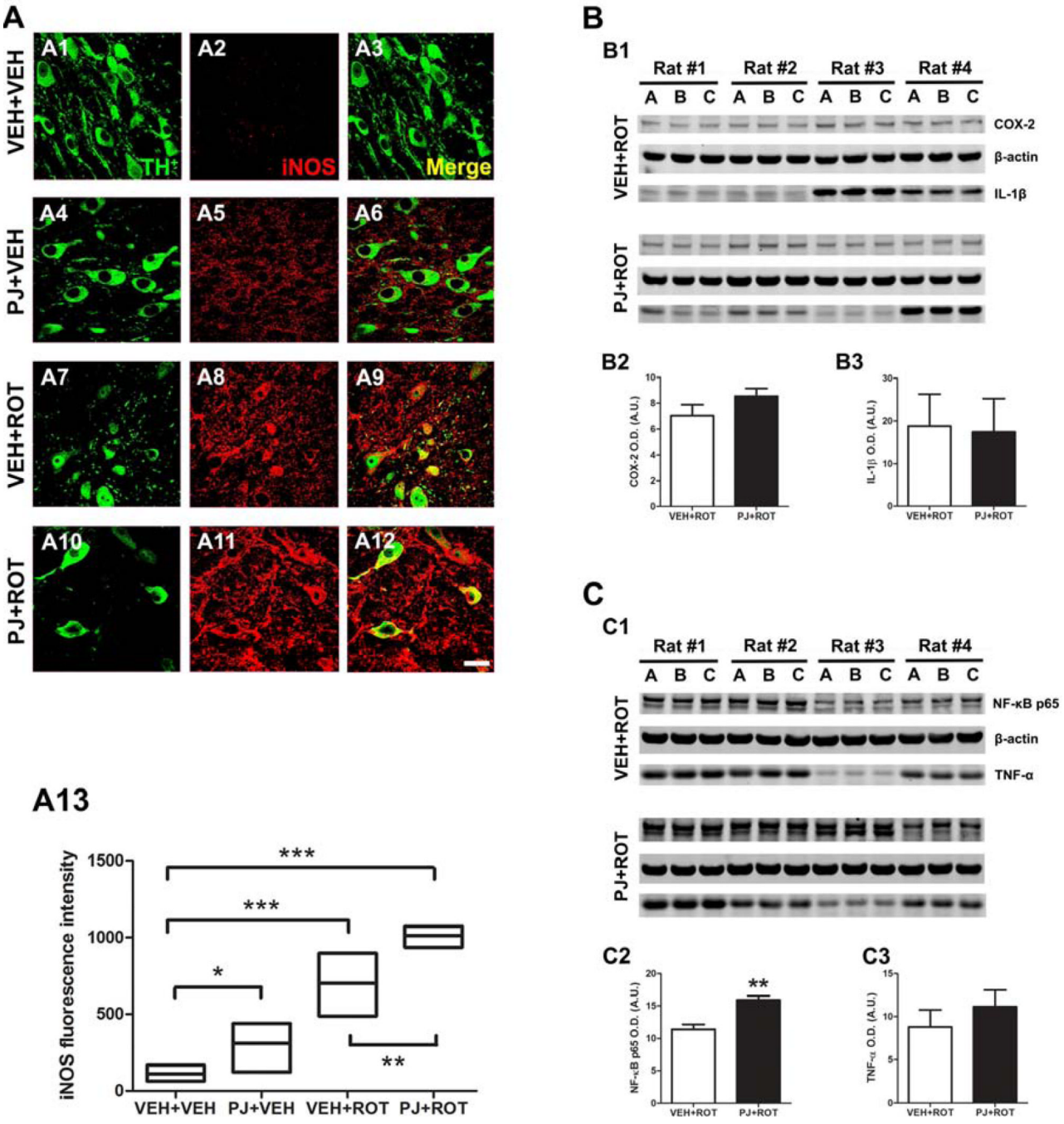


**Figure 8.**

Nigral proinflammatory mediators. Confocal images at 100x revealed an absence of iNOS expression in the vehicle group (***A2***) but oral administration of PJ significantly increased iNOS immunoreactivity (***A5***). Following rotenone injection, a marked expression of iNOS was detected (***A8***) and this effect was even greater when PJ was co-administered with rotenone (***A11***). Quantification of fluorescence levels of iNOS was expressed as the fold increased versus untreated controls (***A13***) and is representative of the average of 200–300 DA neurons corresponding to 5 SN sections per animal. Results are expressed as the mean ± S.E.M. of 4 rats per group. Scale bar = 20 μm. *** $p < 0.001$, * $p < 0.05$ vs VEH+VEH,

Newman-Keuls posthoc test; ** $p < 0.01$ vs VEH+ROT. Representative western blots of different proinflammatory markers in SN brain homogenates (***B*** and ***C***). Densitometric analysis disclosed that the amount of protein for the enzyme COX-2 (~ 74 kDa), the cytokine IL-1β (~ 17 kDa), and TNF-α (~ 17 kDa) remained unchanged (***B2, B3,*** and ***C3***, respectively). Nevertheless, NF-kB p65 (~ 65 kDa) expression levels were significantly enhanced after dietary supplementation with PJ (***C2***). The histogram values represent the mean ± S.E.M in arbitrary units of the optical density of 4 independent measurements in triplicate (A-C are biological replicates). β-Actin was used as a reference control. Significant differences between groups were determined by one-tailed Student's *t*-test. ** $p < 0.01$ and * $p < 0.05$ compared to rotenone.

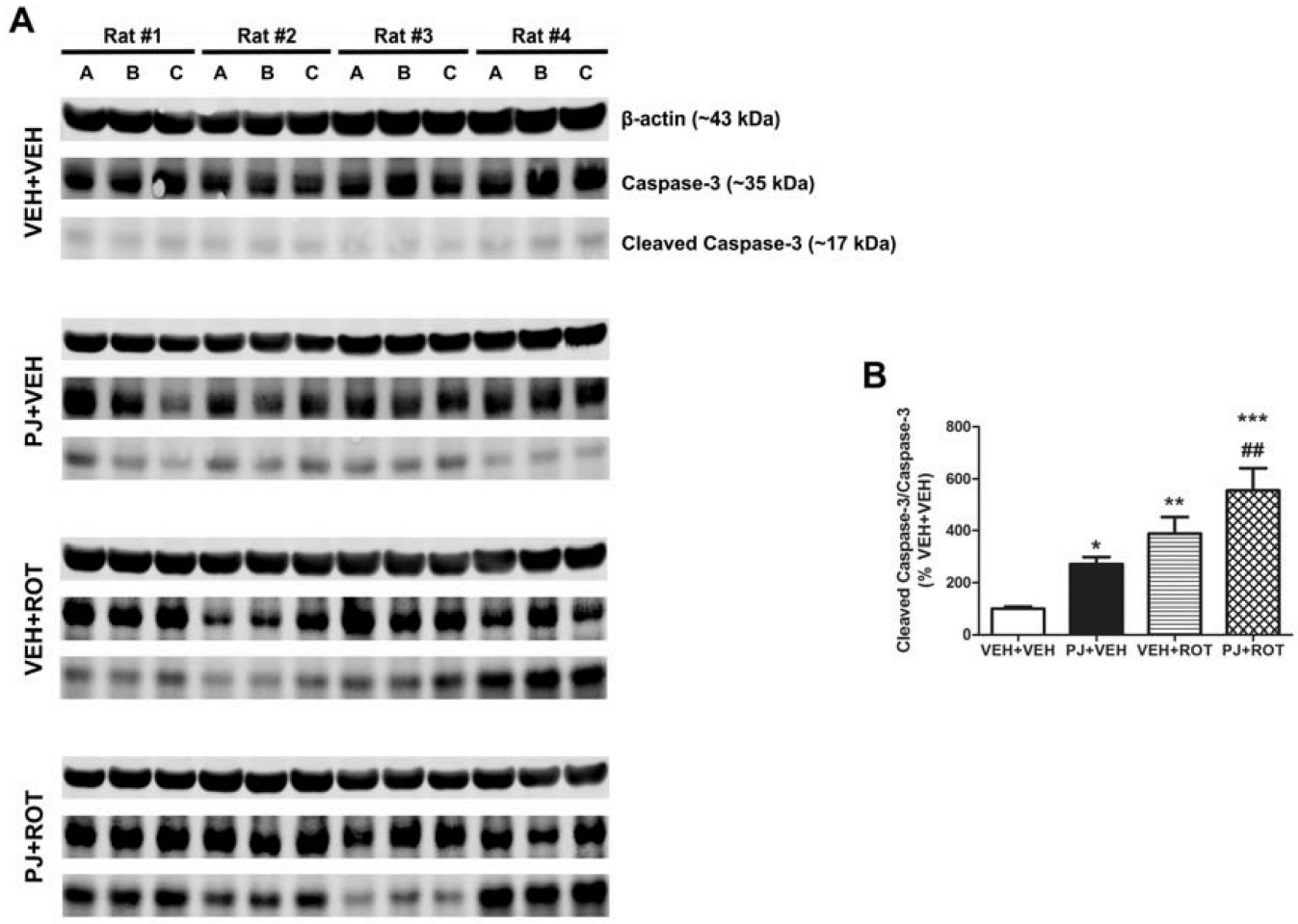


**Figure 9.**

Caspase-3 activation. Ventral midbrain tissue lysate was subjected to western blot with antibodies against procaspase-3 and its active form cleaved caspase-3 (illustrated in ***A***). Semi-quantitative values of activated caspase-3 were determined by optical density measurements on western blot autoradiograms (***B***). Mean values of band densities and their corresponding S.E.M. are obtained from four different animals per group and normalized to percentages of control (VEH+VEH). Significant differences between groups were determined by Newman-Keuls post-hoc test. *** $p < 0.001$, ** $p < 0.01$, and * $p < 0.05$ compared to VEH+VEH. $^{\#\#}$ $p < 0.01$ compared to PJ+VEH.